

Continual Learning with Adaptive Weights (CLAW)

Tameem Adel^{a,*}, Han Zhao^b, Richard E. Turner^{a,c}

^a*Department of Engineering, University of Cambridge, UK*

^b*Machine Learning Department, Carnegie Mellon University*

^c*Microsoft Research, Cambridge, UK*

Abstract

Approaches to continual learning aim to successfully learn a set of related tasks that arrive in an online manner. Recently, several frameworks have been developed which enable deep learning to be deployed in this learning scenario. A key modelling decision is to what extent the architecture should be shared across tasks. On the one hand, separately modelling each task avoids catastrophic forgetting but it does not support transfer learning and leads to large models. On the other hand, rigidly specifying a shared component and a task-specific part enables task transfer and limits the model size, but it is vulnerable to catastrophic forgetting and restricts the form of task-transfer that can occur. Ideally, the network should adaptively identify which parts of the network to share in a data driven way. Here we introduce such an approach called Continual Learning with Adaptive Weights (CLAW), which is based on probabilistic modelling and variational inference. Experiments show that CLAW achieves state-of-the-art performance on six benchmarks in terms of overall continual learning performance, as measured by classification accuracy, and in terms of addressing catastrophic forgetting.

1. Introduction

Continual learning (CL), sometimes called lifelong or incremental learning, refers to an online framework where the knowledge acquired from learning tasks

*Corresponding author

Email address: tah47@cam.ac.uk, tameem.hesham@gmail.com (Tameem Adel)

in the past is kept and accumulated so that it can be reused in the present and future. Data belonging to different tasks could potentially be non i.i.d. (Schlimmer and Fisher, 1986; Sutton and Whitehead, 1993; Ring, 1997; Schmidhuber, 2013; Nguyen et al., 2018; Schmidhuber, 2018). A continual learner must be able to learn a new task, crucially, without forgetting previous tasks (Ring, 1995; Srivastava et al., 2013; Schwarz et al., 2018; Serra et al., 2018; Hu et al., 2019). In addition, CL frameworks should continually adapt to any domain shift occurring across tasks. The learning updates must be incremental – i.e., the model is updated at each task only using the new data and the old model, without access to all previous data (from earlier tasks) – due to speed, security and privacy constraints. A compromise must be found between adapting to new tasks and enforcing stability to preserve knowledge from previous tasks. Excessive adaptation could lead to inadvertent forgetting of how to perform earlier tasks. Indeed, catastrophic forgetting is one of the main pathologies in continual learning (McCloskey and Cohen, 1989; Ratcliff, 1990; Robins, 1993, 1995; French, 1999; Pape et al., 2011; Goodfellow et al., 2014a; Achille et al., 2018; Kemker et al., 2018; Kemker and Kanan, 2018; Diaz-Rodriguez et al., 2018; Zeno et al., 2018; Ahn et al., 2019; Parisi et al., 2019; Pfulb and Gepperth, 2019; Rajasegaran et al., 2019).

Many approaches to continual learning employ an architecture which is divided *a priori* into (i) a slowly evolving, global part; and (ii) a quickly evolving, task-specific, local part. This is one way to enable multi-task transfer whilst mitigating catastrophic forgetting, which has proven to be effective (Rusu et al., 2016b; Fernando et al., 2017; Yoon et al., 2018), albeit with limitations. Specifying *a priori* the shared global, and task-specific local parts in the architecture restricts flexibility. As more complex and heterogeneous tasks are considered, one would like a more flexible, data-driven approach to determine the appropriate amount of sharing across tasks. Here, we aim at automating the architecture adaptation process so that each neuron of the network can either be kept intact, i.e. acting as global, or adapted to the new task locally. Our proposed variational inference framework is flexible enough to learn the range within which the

adaptation parameters can vary. We introduce for each neuron one binary parameter controlling whether or not to adapt, and two parameters to control the magnitude of adaptation. All parameters are learnt via variational inference. We introduce our framework as an expansion of the variational continual learning algorithm (Nguyen et al., 2018), whose variational and sequential Bayesian nature makes it convenient for our modelling and architecture adaptation procedure. Our modelling ideas can also be applied to other continual learning frameworks, see the Appendix for a brief discussion.

We highlight the following contributions: (1) A modelling framework which flexibly automates the adaptation of local and global parts of the (multi-task) continual architecture. This optimizes the tradeoff between mitigating catastrophic forgetting and improving task transfer. (2) A probabilistic variational inference algorithm which supports incremental updates with adaptively learned parameters. (3) The ability to combine our modelling and inference approaches without any significant augmentation of the architecture (no new neurons are needed). (4) State-of-the-art results in six experiments on five datasets, which demonstrate the effectiveness of our framework in terms of overall accuracy and reducing catastrophic forgetting.

1.1. Related Work

We briefly discuss three related approaches to continual learning: (a) regularisation based, (b) architecture based and (c) memory based. We provide more details of related work in Section Appendix A in the Appendix. (a) A complementary approach to CLAW is the regularisation-based approach to balance adaptability with catastrophic forgetting: a level of stability is kept via protecting parameters that greatly influence the prediction against radical changes, while allowing the rest of the parameters to change without restriction (Li and Hoiem, 2016; Lee et al., 2017; Zenke et al., 2017; Chaudhry et al., 2018; Kim et al., 2018; Nguyen et al., 2018; Srivastava et al., 2013; Schwarz et al., 2018; Vuorio et al., 2018; Aljundi et al., 2019c). The elastic weight consolidation (EWC) algorithm by Kirkpatrick et al. (2017) is a seminal example, where a

quadratic penalty is imposed on the difference between parameter values of the old and new tasks. One limitation is the high level of hand tuning required. (b) The architecture-based approach aims to deal with stability and adaptation issues by a fixed division of the architecture into global and local parts (Rusu et al., 2016b; Fernando et al., 2017; Shin et al., 2017; Kaplanis et al., 2018; Xu and Zhu, 2018; Yoon et al., 2018; Li et al., 2019b). (c) The memory-based approach relies on episodic memory to store data (or pseudo-data) from previous tasks (Ratcliff, 1990; Robins, 1993, 1995; Thrun, 1996; Schmidhuber, 2013; Hattori, 2014; Mocanu et al., 2016; Rebuffi et al., 2017; Kamra et al., 2017; Shin et al., 2017; Rolnick et al., 2018; van de Ven and Tolias, 2018; Wu et al., 2018; Titsias et al., 2019). Limitations include overheads for tasks such as data storage, replay, and optimisation to select (or generate) the points. **CLAW** can as well be seen as a combination of a regularisation-based approach (the variational inference mechanism) and a modelling approach which automates the architecture building process in a data-driven manner, avoiding the overhead resulting from either storing or generating data points from previous tasks. **CLAW** is also orthogonal to (and simple to combine with, if needed) memory-based methods.

2. Background on Variational Continual Learning (VCL)

In this paper, we use Variational Continual Learning (VCL, Nguyen et al., 2018) as the underlying continual learning framework. However, our methods apply to other frameworks, see Appendix (Section Appendix A.1). VCL is a variational Bayesian framework where the posterior of the model parameters θ is learnt and updated continually from a sequence of T datasets, $\{\mathbf{x}_t^{(n)}, \mathbf{y}_t^{(n)}\}_{n=1}^{N_t}$, where $t = 1, 2, \dots, T$ and N_t is the size of the dataset associated with the t -th task. More specifically, denote by $p(\mathbf{y}|\theta, \mathbf{x})$ the probability distribution returned by a discriminative classifier with input \mathbf{x} , output \mathbf{y} and parameters θ . For $\mathcal{D}_t = \{\mathbf{y}_t^{(n)}\}_{n=1}^{N_t}$, we approximate the intractable posterior $p(\theta|\mathcal{D}_{1:t})$ after

observing the first t datasets via a tractable variational distribution q_t as:¹

$$\mathbf{q}_t(\boldsymbol{\theta}) \approx \frac{1}{Z_t} \mathbf{q}_{t-1}(\boldsymbol{\theta}) p(\mathcal{D}_t|\boldsymbol{\theta}), \quad (1)$$

where \mathbf{q}_0 is the prior p , $p(\mathcal{D}_t|\boldsymbol{\theta}) = \prod_{n=1}^{N_t} p(\mathbf{y}_t^{(n)}|\boldsymbol{\theta}, \mathbf{x}_t^{(n)})$, and Z_t is the normalization constant which does not depend on $\boldsymbol{\theta}$ but only on the data \mathcal{D} . This framework allows the approximate posterior $\mathbf{q}_t(\boldsymbol{\theta})$ to be updated incrementally from the previous approximate posterior $\mathbf{q}_{t-1}(\boldsymbol{\theta})$ in an online fashion. In VCL, the approximation in (1) is performed by minimizing the following KL-divergence over a family \mathcal{Q} of tractable distributions:

$$\mathbf{q}_t(\boldsymbol{\theta}) = \operatorname{argmin}_{\mathbf{q} \in \mathcal{Q}} \operatorname{KL}\left(\mathbf{q}(\boldsymbol{\theta}) \parallel \frac{1}{Z_t} \mathbf{q}_{t-1}(\boldsymbol{\theta}) p(\mathcal{D}_t|\boldsymbol{\theta})\right). \quad (2)$$

This framework can be enhanced to further mitigate catastrophic forgetting by using a coreset (Nguyen et al., 2018), i.e. a representative set of data from previously observed tasks that can serve as memory and can be revisited before making a decision. As discussed in the Related Work, this leads to overhead costs of memory and optimisation (selecting most representative data points). Previous work on VCL considered simple models without automatic architecture building or adaptation.

3. Our CLAW Approach

In earlier CL approaches, the parts of the network architecture that are shared among the learnt tasks are designated *a priori*. To alleviate this rigidity and to effectively balance adaptation and stability, we propose a multi-task, continual model in which the adaptation of the architecture is data-driven by learning which neurons need to be adapted as well as the maximum adaptation capacity for each. All the model parameters (including those used for adaptation) are estimated via an efficient variational inference algorithm which

¹Here we suppress the dependence on the inputs in $p(\boldsymbol{\theta}|\mathcal{D}_{1:t})$ and $p(\mathcal{D}_t|\boldsymbol{\theta})$ to lighten notation.

incrementally learns from data of the successive tasks, without a need to store (nor generate) data from previous tasks and with no expansion in the network size.

3.1. Modelling

With model parameters θ , the overall variational objective we aim at maximising at task with index \mathbf{t} is equivalent to the following online marginal likelihood:

$$\mathcal{L}(\theta) = -\text{KL}(\mathbf{q}_{\mathbf{t}}(\theta) \parallel \mathbf{q}_{\mathbf{t}-1}(\theta)) + \sum_{n=1}^{N_{\mathbf{t}}} \mathbb{E}_{\mathbf{q}_{\mathbf{t}}(\theta)} [\log p(\mathbf{y}^{(n)} | \mathbf{x}^{(n)}, \theta)]. \quad (3)$$

We propose a framework where the architecture, whose parameters are θ , is flexibly adapted based on the available tasks, via a learning procedure that will be described below. With each task, we automate the adaptation of the neuron contributions. Both the adaptation decisions (i.e. whether or not to adapt) and the maximum allowed degree of adaptation for every neuron are learnt. We refer to the binary adaptation variable as α . There is another variable \mathbf{s} that is learnt in a multi-task fashion to control the maximum degree of adaptation, such that the expression $\mathbf{b} = \frac{\mathbf{s}}{1+e^{-\mathbf{a}}} - 1$ limits how far the task-specific weights can differ from the global weights, in case the respective neuron is to be adapted. The parameter \mathbf{a} depicts unconstrained adaptation, as described later.²

We illustrate the proposed model to perform this adaptation by learning the probabilistic contributions of the different neurons within the network architecture on a task-by-task basis. We follow this with the inference details. Steps of the proposed modeling are listed as follows:

- For a task T , the classifier that we are modeling outputs: $\sum_{n=1}^{N_T} [\log p(\mathbf{y}^{(n)} | \mathbf{x}^{(n)}, \mathbf{w}^T)]$

²We learn parameters α , \mathbf{s} and \mathbf{a} , with corresponding \mathbf{b} , for each neuron but we avoid using the neuron indices here, as well as in other locations like (4), (6) and (7), for better readability.

- The task-specific weights \mathbf{w}^T can be expressed in terms of their global counterparts as follows:

$$\mathbf{w}^T = (1 + \mathbf{b}^T \boldsymbol{\alpha}^T) \circ \mathbf{w}. \quad (4)$$

The symbol \circ denotes an element-wise (Hadamard) multiplication.

- For each task T and each neuron \mathbf{j} at layer \mathbf{i} , $\alpha_{\mathbf{i},\mathbf{j}}^T$ is a binary variable which indicates whether the corresponding weight is adapted ($\alpha_{\mathbf{i},\mathbf{j}}^T = 1$) or unadapted ($\alpha_{\mathbf{i},\mathbf{j}}^T = 0$). Initially assume that the adaptation probability $\alpha_{\mathbf{i},\mathbf{j}}^T$ follows a Bernoulli distribution with probability $\mathbf{p}_{\mathbf{i},\mathbf{j}}$ ³, $\alpha_{\mathbf{i},\mathbf{j}}^T \sim \text{Bernoulli}(\mathbf{p}_{\mathbf{i},\mathbf{j}})$. Since this Bernoulli is not straightforward to optimise, and to adopt a scalable inference procedure based on continuous latent variables, we replace this Bernoulli with a Gaussian that has an equivalent mean and variance from which we draw $\alpha_{\mathbf{i},\mathbf{j}}^T$. For the sake of attaining higher fidelity than what is granted by a standard Gaussian, we base our inference on a variational Gaussian estimation. Though in a context different from continual learning and with different estimators, the idea of replacing Bernoulli with an equivalent Gaussian has proven to be effective with dropout (Srivastava et al., 2014; Kingma et al., 2015).

The approximation of the Bernoulli distribution by the corresponding Gaussian distribution is achieved by matching the mean and variance. The mean and variance of the Bernoulli distribution are $\mathbf{p}_{\mathbf{i},\mathbf{j}}$, $\mathbf{p}_{\mathbf{i},\mathbf{j}}(1 - \mathbf{p}_{\mathbf{i},\mathbf{j}})$, respectively. A Gaussian distribution with the same mean and variance is used to fit $\alpha_{\mathbf{i},\mathbf{j}}^T$.

$$\alpha_{\mathbf{i},\mathbf{j}}^T \sim \mathcal{N}(\mathbf{p}_{\mathbf{i},\mathbf{j}}, \mathbf{p}_{\mathbf{i},\mathbf{j}}(1 - \mathbf{p}_{\mathbf{i},\mathbf{j}})). \quad (5)$$

- The variable \mathbf{b}^T controls the strength of the adaptation and it limits the range of adaptation via:

$$1 + \mathbf{b}^T = \frac{\mathbf{s}}{1 + e^{-\mathbf{a}^T}}. \quad (6)$$

³There can be a parameter $\mathbf{p}_{\mathbf{i}}$ per layer \mathbf{i} instead of one $\mathbf{p}_{\mathbf{i},\mathbf{j}}$ for each neuron \mathbf{j} at each layer \mathbf{i} , but we opt for the latter for the sake of gaining further adaptation flexibility.

So that the maximum adaptation is \mathbf{s} . The variable \mathbf{a}^T is an unconstrained adaptation value, similar to that in (Swietojanski and Renals, 2014). The addition of 1 is to facilitate the usage of a probability distribution while still keeping an adaptation range allowing for the attenuation or amplification of each neuron’s contribution.

- Before facing the first dataset and learning task $\mathbf{t} = 1$, the prior on the weights $\mathbf{q}_0(\mathbf{w}) = \mathbf{p}(\mathbf{w})$ is chosen to be a log-scale prior, which can be expressed as: $\mathbf{p}(\log |\mathbf{w}|) \propto \mathbf{c}$, where \mathbf{c} is a constant. The log-scale prior can alternatively be described as:

$$\mathbf{p}(|\mathbf{w}|) \propto \frac{1}{|\mathbf{w}|}. \quad (7)$$

At a high level, adapting neuron contributions can be seen as a generalisation of attention mechanisms in the context of continual learning. Applying this adaptation procedure to the input leads to an attention mechanism. However, our approach is more general since we do not apply it only to the very bottom (i.e. input) layer, but throughout the whole network. We next show how our variational inference mechanism enables us to learn the adaptation parameters.

3.2. Inference

We describe the details related to the proposed variational inference mechanism. The adaptation parameters are included within the variational parameters.

The (unadapted version of the) model parameters $\boldsymbol{\theta}$ consist of the weight vectors \mathbf{w} . To automate adaptation, we perform inference on $\mathbf{p}_{i,j}$, which would have otherwise been a hyperparameter of the prior (Louizos et al., 2017; Molchanov et al., 2017; Ghosh et al., 2018). Multiplying \mathbf{w} by $(1 + \mathbf{b}\boldsymbol{\alpha})$ where $\boldsymbol{\alpha}$ is distributed according to (5), then from (4) with random noise variable $\epsilon \sim \mathcal{N}(0, 1)$:

$$\begin{aligned} \mathbf{w}_{i,j}^T &= \gamma_{i,j}(1 + \mathbf{b}_{i,j}\mathbf{p}_{i,j} + \mathbf{b}_{i,j}\sqrt{\mathbf{p}_{i,j}(1 - \mathbf{p}_{i,j})}\epsilon), \\ \mathbf{q}(\mathbf{w}_{i,j}|\gamma_{i,j}) &\sim \mathcal{N}\left(\gamma_{i,j}(1 + \mathbf{b}_{i,j}\mathbf{p}_{i,j}), \mathbf{b}_{i,j}^2 \gamma_{i,j}^2 \mathbf{p}_{i,j}(1 - \mathbf{p}_{i,j})\right). \end{aligned} \quad (8)$$

From (7) and (8), the corresponding KL-divergence between the variational posterior of \mathbf{w} , $\mathbf{q}(\mathbf{w}|\gamma)$ and the prior $\mathbf{p}(\mathbf{w})$ is as follows. The subscripts are removed when \mathbf{q} in turn is used as a subscript for improved readability. The variational parameters are $\gamma_{i,j}$ and $\mathbf{p}_{i,j}$.

$$\begin{aligned} \text{KL}\left(\mathbf{q}(\mathbf{w}_{i,j}|\gamma_{i,j}) \parallel \mathbf{p}(\mathbf{w}_{i,j})\right) &= \mathbb{E}_{\mathbf{q}(\mathbf{w}|\gamma)} \log[\mathbf{q}(\mathbf{w}_{i,j}|\gamma_{i,j})/\mathbf{p}(\mathbf{w}_{i,j})] = \\ \mathbb{E}_{\mathbf{q}(\mathbf{w}|\gamma)} \log \mathbf{q}(\mathbf{w}_{i,j}|\gamma_{i,j}) - \mathbb{E}_{\mathbf{q}(\mathbf{w}|\gamma)} \log \mathbf{p}(\mathbf{w}_{i,j}) &= -\mathbf{H}(\mathbf{q}(\mathbf{w}_{i,j}|\gamma_{i,j})) - \mathbb{E}_{\mathbf{q}(\mathbf{w}|\gamma)} \log \mathbf{p}(\mathbf{w}_{i,j}) \end{aligned} \quad (9)$$

$$= -0.5\left(1 + \log(2\pi) + \log(\mathbf{b}_{i,j}^2 \mathbf{p}_{i,j}(1 - \mathbf{p}_{i,j}))\right) - \mathbb{E}_{\mathbf{q}(\mathbf{w}|\gamma)} \log \frac{1}{|\boldsymbol{\epsilon}|} \quad (10)$$

$$= -\log \mathbf{b}_{i,j} - 0.5 \log \mathbf{p}_{i,j} - 0.5 \log(1 - \mathbf{p}_{i,j}) + \mathbf{c} + \mathbb{E}_{\mathbf{q}(\mathbf{w}|\gamma)} \log |\boldsymbol{\epsilon}|, \quad (11)$$

where the switch from (9) to (10) is due to the entropy computation (Bernardo and Smith, 2000) of the Gaussian $\mathbf{q}(\mathbf{w}_{i,j}|\gamma_{i,j})$ defined in (8). The switch from (10) to (11) is due to using a log-scale prior, similar to Appendix C in (Kingma et al., 2015) and to Section 4.2 in (Molchanov et al., 2017). $\mathbb{E}_{\mathbf{q}(\mathbf{w}|\gamma)} \log |\boldsymbol{\epsilon}|$ is computed via an accurate approximation similar to equation (14) in (Molchanov et al., 2017), with slightly different values of k_1 , k_2 and k_3 . This is a very close approximation via numerically pre-computing $\mathbb{E}_{\mathbf{q}(\mathbf{w}|\gamma)} \log |\boldsymbol{\epsilon}|$ using a third degree polynomial (Kingma et al., 2015; Molchanov et al., 2017).

This is the form of the KL-divergence between the approximate posterior after the first task and the prior. Afterwards, it is straightforward to see how this KL-divergence applies for the subsequent tasks in a manner similar to (2), but while taking into account the new posterior form and original prior.

The KL-divergence expression derived in (11) is to be minimised. By minimising (11) with respect to $\mathbf{p}_{i,j}$ and then using samples from the respective distributions to assign values to $\boldsymbol{\alpha}_{i,j}$, adapted contributions of each neuron \mathbf{j} at each layer \mathbf{i} of the network are learnt per task. Values of $\mathbf{p}_{i,j}$ are constrained between 0 and 1 during training via projected gradient descent.

3.2.1. Learning the maximum adaptation values

Using (6) to express the value of $\mathbf{b}_{i,j}$, and neglecting the constant term therein since it does not affect the optimisation, the KL-divergence in (11) is equivalent to:

$$\begin{aligned} \text{KL}(\mathbf{q}(\mathbf{w}_{i,j}|\gamma_{i,j}) \parallel \mathbf{p}(\mathbf{w}_{i,j})) &\approx \\ -\log \mathbf{s}_{i,j} + \log(1 + e^{-\mathbf{a}_{i,j}}) - 0.5 \log \mathbf{p}_{i,j} - 0.5 \log(1 - \mathbf{p}_{i,j}) + \mathbf{c} + \mathbb{E}_{\mathbf{q}(\mathbf{w}_{i,j})} \log |\epsilon|. \end{aligned} \quad (12)$$

Values of $\mathbf{a}_{i,j}$ are straightforwardly learnt by minimising (12) with respect to $\mathbf{a}_{i,j}$. This subsection explains how to learn the maximum adaptation variable $\mathbf{s}_{i,j}$. Values of the maximum $\mathbf{s}_{i,j}$ of the logistic function defined in (6) are learnt from multiple tasks. For each neuron \mathbf{j} at layer \mathbf{i} , there is a general value $\mathbf{s}_{i,j}$ and another value that is specific for each task \mathbf{t} , referred to as $\mathbf{s}_{i,j,t}$. This is similar to the meta-learning procedure proposed in (Finn et al., 2017). The following procedure to learn \mathbf{s} is performed for each task \mathbf{t} such that: (i) the optimisation performed to learn a task-specific value $\mathbf{s}_{i,j,t}$ benefits from the warm initialisation with the general value $\mathbf{s}_{i,j}$ rather than a random initial condition; and then (ii) the new information obtained from the current task \mathbf{t} is ultimately reflected back to update the general value $\mathbf{s}_{i,j}$.

- First divide the sample N_t into two halves. For the first half, depart from the general value of $\mathbf{s}_{i,j}$ as an initial condition, and use the assigned data examples from task \mathbf{t} to learn the task-specific values $\mathbf{s}_{i,j,t}$ for the current task \mathbf{t} . For neuron \mathbf{j} at layer \mathbf{i} , refer to the second term in (3), $\sum_{n=1}^{N_t} \mathbb{E}_{\mathbf{q}_t(\boldsymbol{\theta})} [\log p(\mathbf{y}^{(n)}|\mathbf{x}^{(n)}, \boldsymbol{\theta})]$ as $\mathbf{f}_t(\mathbf{x}, \mathbf{y}, \mathbf{s}_{i,j})$. The set of parameters $\boldsymbol{\theta}$ contains \mathbf{s} as well as other parameters, but we focus here on \mathbf{s} in the \mathbf{f} notation since the following procedure is developed to optimise \mathbf{s} . Also, refer to the loss of the (classification) function \mathbf{f} as $\mathbf{Err}(\mathbf{f}) = \text{CE}(\mathbf{f}(\mathbf{x}, \boldsymbol{\theta})\|\mathbf{y})$, where CE stands for the cross-entropy:

$$\mathbf{s}_{i,j,t} = \mathbf{s}_{i,j} - \frac{2\omega_1}{N_t} \nabla_{\mathbf{s}_{i,j}} \sum_{d=1}^{N_t/2} \mathbf{Err}(\mathbf{f}_t(\mathbf{x}_d, \mathbf{y}_d, \mathbf{s}_{i,j})). \quad (13)$$

- Now use the second half of the data from task \mathbf{t} to update the general learnt value $\mathbf{s}_{\mathbf{i},\mathbf{j}}$:

$$\mathbf{s}_{\mathbf{i},\mathbf{j}} = \mathbf{s}_{\mathbf{i},\mathbf{j}} - \frac{2\omega_2}{N_t} \nabla_{\mathbf{s}_{\mathbf{i},\mathbf{j}}} \sum_{d=1+N_t/2}^{N_t} \mathbf{Err}(\mathbf{f}_t(\mathbf{x}_d, \mathbf{y}_d, \mathbf{s}_{\mathbf{i},\mathbf{j},\mathbf{t}})). \quad (14)$$

Where ω_1 and ω_2 are step-size parameters.

When testing on samples from task \mathbf{t} after having faced future tasks $\mathbf{t} + 1, \mathbf{t} + 2, \dots$, the value of $\mathbf{s}_{\mathbf{i},\mathbf{j}}$ used is the learnt $\mathbf{s}_{\mathbf{i},\mathbf{j},\mathbf{t}}$. There is only one value per neuron, so the overhead resulting from storing such values is negligible.

The key steps of the algorithm are listed in Algorithm 1.

Algorithm 1 Continual Learning with Adaptive Weights (CLAW)

Input: A sequence of T datasets, $\{\mathbf{x}_t^{(n)}, \mathbf{y}_t^{(n)}\}_{n=1}^{N_t}$, where $t = 1, 2, \dots, T$ and N_t is the size of the dataset associated with the t -th task.

Output: $\mathbf{q}_t(\boldsymbol{\theta})$, where $\boldsymbol{\theta}$ are the model parameters.

Initialise all $\mathbf{p}(|\mathbf{w}_{\mathbf{i},\mathbf{j}}|)$ with a log-scale prior, as in (7).

for $t = 1 \dots T$ **do**

 Disclose the dataset $\{\mathbf{x}_t^{(n)}, \mathbf{y}_t^{(n)}\}_{n=1}^{N_t}$ for the current task \mathbf{t} .

for $\mathbf{i} = 1 \dots \# \text{ layers}$ **do**

for $\mathbf{j} = 1 \dots \# \text{ neurons at layer } \mathbf{i}$ **do**

 Compute $\mathbf{p}_{\mathbf{i},\mathbf{j}}$ using stochastic gradient descent on (11).

 Compute $\mathbf{s}_{\mathbf{i},\mathbf{j},\mathbf{t}}$ using (13).

 Update the corresponding general value $\mathbf{s}_{\mathbf{i},\mathbf{j}}$ using (14).

end for

end for

end for

At task \mathbf{t} , the algorithmic complexity of a single joint update of the parameters $\boldsymbol{\theta}$ based on the additive terms in (12) is $O(MELD^2)$, where L is the number of layers in the network, D is the (largest) number of neurons within a single layer, E is the number of samples taken from the random noise variable ϵ , and M is the minibatch size. Each α is obtained by taking one sample from

the corresponding \mathbf{p} , so that does not result in an overhead in terms of the complexity.

4. Experiments

Our experiments mainly aim at evaluating the following: (i) the overall performance of the introduced **CLAW**, depicted by the average classification accuracy over all the tasks; (ii) the extent to which catastrophic forgetting can be mitigated when deploying **CLAW**; and (iii) the achieved degree of positive forward transfer. The experiments demonstrate the effectiveness of **CLAW** in achieving state-of-the-art continual learning results measured by classification accuracy and by the achieved reduction in catastrophic forgetting. We also perform ablations in Section Appendix D in the Appendix which exhibit the relevance of each of the proposed adaptation parameters.

We perform six experiments on five datasets. The datasets in use are: MNIST (LeCun et al., 1998), notMNIST (Butalov, 2011), Fashion-MNIST (Xiao et al., 2017), Omniglot (Lake et al., 2011) and CIFAR-100 (Krizhevsky and Hinton, 2009). We compare the results obtained by **CLAW** to six different state-of-the-art continual learning algorithms: the VCL algorithm (Nguyen et al., 2018) (original form and one with a coreset), the elastic weight consolidation (EWC) algorithm (Kirkpatrick et al., 2017), the progress and compress (P&C) algorithm (Schwarz et al., 2018), the reinforced continual learning (RCL) algorithm (Xu and Zhu, 2018), the one referred to as functional regularisation for continual learning (FRCL) using Gaussian processes (Titsias et al., 2019) and the learn-to-grow (LTG) algorithm (Li et al., 2019b).

4.1. Overall Classification Accuracy

Our main metric is the all-important classification accuracy. We consider six continual learning experiments, based on the MNIST, notMNIST, Fashion-MNIST, Omniglot and CIFAR-100 datasets. The introduced **CLAW** is compared to two VCL versions: VCL with no coreset and VCL with a 200-point coreset assembled by the K-center method (Nguyen et al., 2018), EWC, P&C, RCL,

FRCL (its TR version) and LTG⁴. All the reported classification accuracy values reflect the average classification accuracy over all tasks the learner has trained on so far. More specifically, assume that the continual learner has just finished training on a task t , then the reported classification accuracy at time t is the average accuracy value obtained from testing on equally sized sets each belonging to one of the tasks $1, 2, \dots, t$. For all the classification experiments, statistics reported are averages of ten repetitions. Statistical significance and standard error of the average classification accuracy obtained after completing the last two tasks of each experiment are displayed in Section Appendix B in the Appendix.

As can be seen in Figure 1, CLAW achieves state-of-the-art classification accuracy in all the six experiments. The minibatch size is 128 for Split MNIST and 256 for all the other experiments. More detailed descriptions of the results of every experiment are given next:

Permuted MNIST Using MNIST, Permuted MNIST is a standard continual learning benchmark (Goodfellow et al., 2014a; Kirkpatrick et al., 2017; Zenke et al., 2017). For each task t , the corresponding dataset is formed by performing a fixed random permutation process on labeled MNIST images. This random permutation is unique per task, i.e. it differs for each task. For the hyperparameter λ of EWC, which controls the overall contribution from previous data, we experimented with two values, $\lambda = 1$ and $\lambda = 100$. We report the latter since it has always outperformed EWC with $\lambda = 1$ in this experiment. EWC with $\lambda = 100$ has also previously produced the best EWC classification results (Nguyen et al., 2018). In this experiment, fully connected single-head networks with two hidden layers are used. There are 100 hidden units in each layer, with ReLU activations. Adam (Kingma and Ba, 2015) is the optimiser used in the 6 experiments with $\eta = 0.001$, $\beta_1 = 0.9$ and $\beta_2 = 0.999$. Further

⁴Whenever there is no validation process performed to indicate the hyperparameter values of competitors or characteristics of neural network architectures, this is done for the sake of comparing on common ground with the best settings, as specified in the respective papers.

experimental details are given in Section Appendix C in the Appendix. Results of the accumulated classification accuracy, averaged over tasks, on a test set are displayed in Figure 1a. After 10 tasks, **CLAW** achieves significantly (check the Appendix) higher classification results than all the competitors.

Split MNIST In this MNIST based experiment, five binary classification tasks are processed in the following sequence: 0/1, 2/3, 4/5, 6/7, and 8/9 (Zenke et al., 2017). The architecture used consists of fully connected multi-head networks with two hidden layers, each consisting of 256 hidden units with ReLU activations. As can be seen in Figure 1b, **CLAW** achieves the highest classification accuracy.

Split notMNIST It contains 400,000 training images, and the classes are 10 characters, from A to J. Each image consists of one character, and there are different font styles. The five binary classification tasks are: A/F, B/G, C/H, D/I, and E/J. The networks used here contain four hidden layers, each containing 150 hidden units with ReLU activations. **CLAW** achieves a clear improvement in classification accuracy over competitors (Figure 1c).

Split Fashion-MNIST Fashion-MNIST is a dataset whose size is the same as MNIST but it is based on different (and more challenging) 10 classes. The five binary classification tasks here are: T-shirt/Trouser, Pullover/Dress, Coat/Sandals, Shirt/Sneaker, and Bag/Ankle boots. The architecture used is the same as in Split notMNIST. In most of the continual learning tasks (including the more significant, later ones) **CLAW** achieves a clear classification improvement (Figure 1d).

Omniglot This is a sequential learning task of handwritten characters of 50 alphabets (a total of over 1,600 characters with 20 examples each) belonging to the Omniglot dataset (Lake et al., 2011). We follow the same way via which this task has been used in continual learning before (Schwarz et al., 2018; Titsias et al., 2019); handwritten characters from each alphabet constitute a separate task. We thus have 50 tasks, which also allows to evaluate the scalability of the frameworks in comparison. The model used is a CNN. To deal with the convolutions in **CLAW**, we used the idea proposed and referred to as the local

reparameterisation trick by Kingma et al. (2014, 2015), where a single global parameter is employed per neuron activation in the variational distribution, rather than employing parameters for every constituent weight element⁵. Further details about the CNN used are given in Section Appendix C. The automatically adaptable **CLAW** achieves better classification accuracy (Figure 1e).

CIFAR-100 This dataset consists of 60,000 colour images of size 32×32 . It contains 100 classes, with 600 images per class. We use a split version CIFAR-100. Similar to Lopez-Paz and Ranzato (2017), we perform a 20-task experiment with a disjoint subset of five classes per task. **CLAW** achieves significantly higher classification accuracy (Figure 1f) -also higher than the previous state of the art on CIFAR-100 by Kemker and Kanan (2018). Details of the used CNN are in Section Appendix C.

A conclusion that can be taken from Figure 1(a-f) is that **CLAW** consistently achieves state-of-the-art results (in all the 6 experiments). It can also be seen that **CLAW** scales well. For instance, the difference between **CLAW** and the best competitor is more significant with Split notMNIST than it is with the first two experiments, which are based on the smaller and less challenging MNIST. Also, **CLAW** achieves good results with Omniglot and CIFAR-100.

4.2. Catastrophic Forgetting

To assess catastrophic forgetting, we show how the accuracy on the initial task varies over the course of the training procedure on the remaining tasks (Schwarz et al., 2018). Since Omniglot (and CIFAR-100) contain a larger number of tasks: 50 (20) tasks, i.e. 49 (19) remaining tasks after the initial task, this setting is more relevant for Omniglot and CIFAR-100. We nonetheless display the results for Split MNIST, Split notMNIST, Split Fashion-MNIST, Omniglot and CIFAR-100. As can be seen in Figure 2, **CLAW** (at times jointly) achieves state-of-the-art performance retention degrees. Among the competitors, P&C and LTG also achieve high performance retention degrees.

⁵For more details, see Section 2.3 in (Kingma et al., 2015).

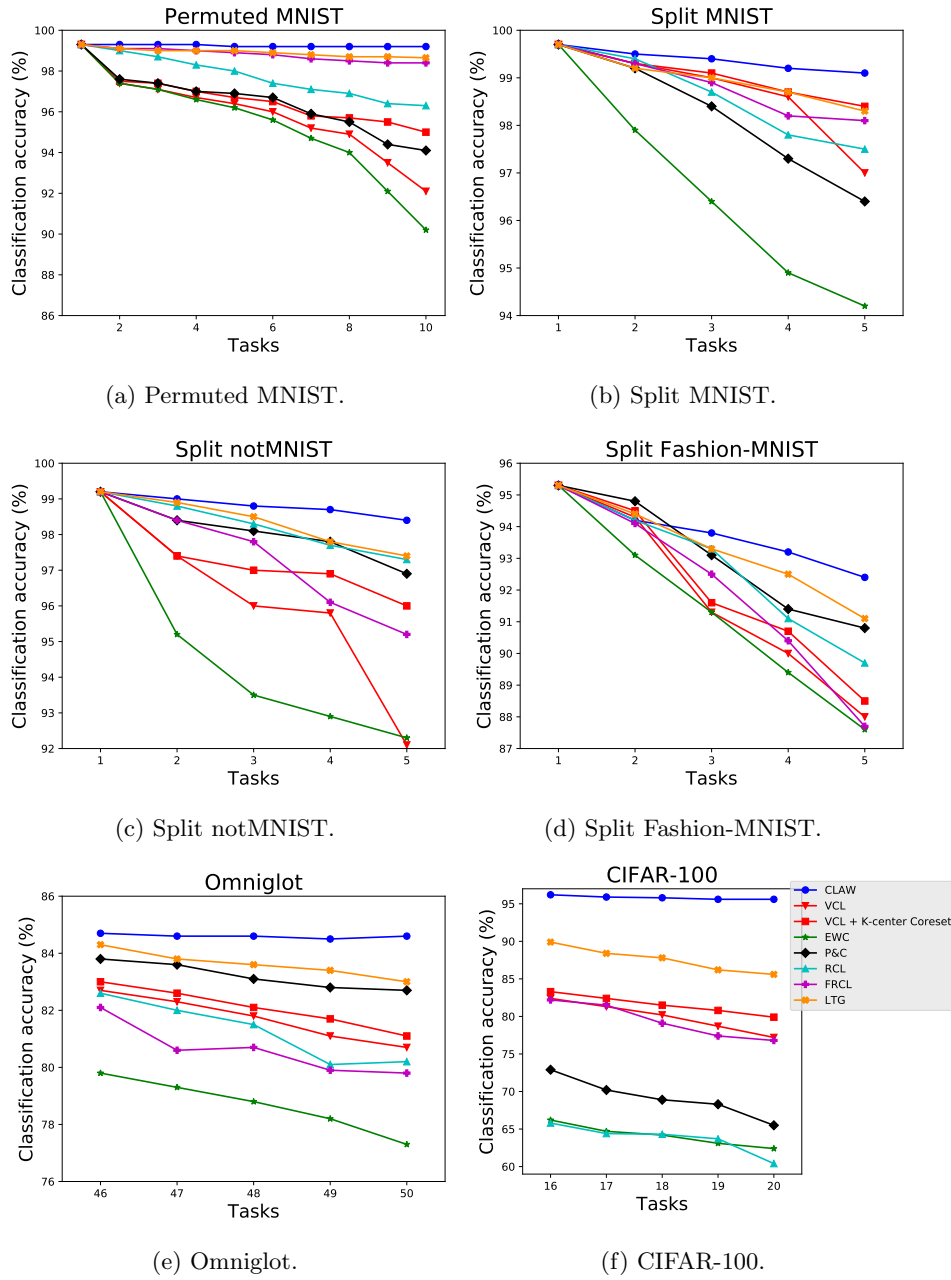


Figure 1: Average test classification accuracy vs. the number of observed tasks in 6 experiments. **CLAW** achieves significantly higher classification results than the competing continual learning frameworks. Statistical significance values are presented in Section Appendix B in the Appendix. The value of λ for EWC is 10,000 in (c), and 100 in the other experiments. Best viewed in colour.

An empirical conclusion that can be made out of this and the previous experiment, is that **CLAW** achieves better overall continual learning results, partially thanks to the way it addresses catastrophic forgetting. The idea of adapting the architecture by adapting the contributions of neurons of each layer also seems to be working well with datasets like Omniglot and CIFAR-100, giving directions for imminent future work where **CLAW** can be extended for other application areas based on CNNs.

4.3. Positive Forward Transfer

The purpose of this experiment is to assess the impact of learning previous tasks on the current task. In other words, we want to evaluate whether an algorithm avoids negative transfer, by evaluating the relative performance achieved on a unique task after learning a varying number of previous tasks (Schwarz et al., 2018). From Figure 3, we can see that **CLAW** achieves state-of-the-art results in 4 out of the 5 experiments (at par in the fifth) in terms of avoiding negative transfer.

5. Conclusion

We introduced a continual learning framework which learns how to adapt its architecture from the tasks and data at hand, based on variational inference. Rather than rigidly dividing the architecture into shared and task-specific parts, our approach adapts the contributions of each neuron. We achieve that without having to expand the architecture with new layers or new neurons. Results of six different experiments on five datasets demonstrate the strong empirical performance of the introduced framework, in terms of the average overall continual learning accuracy and forward transfer, and also in terms of effectively alleviating catastrophic forgetting.

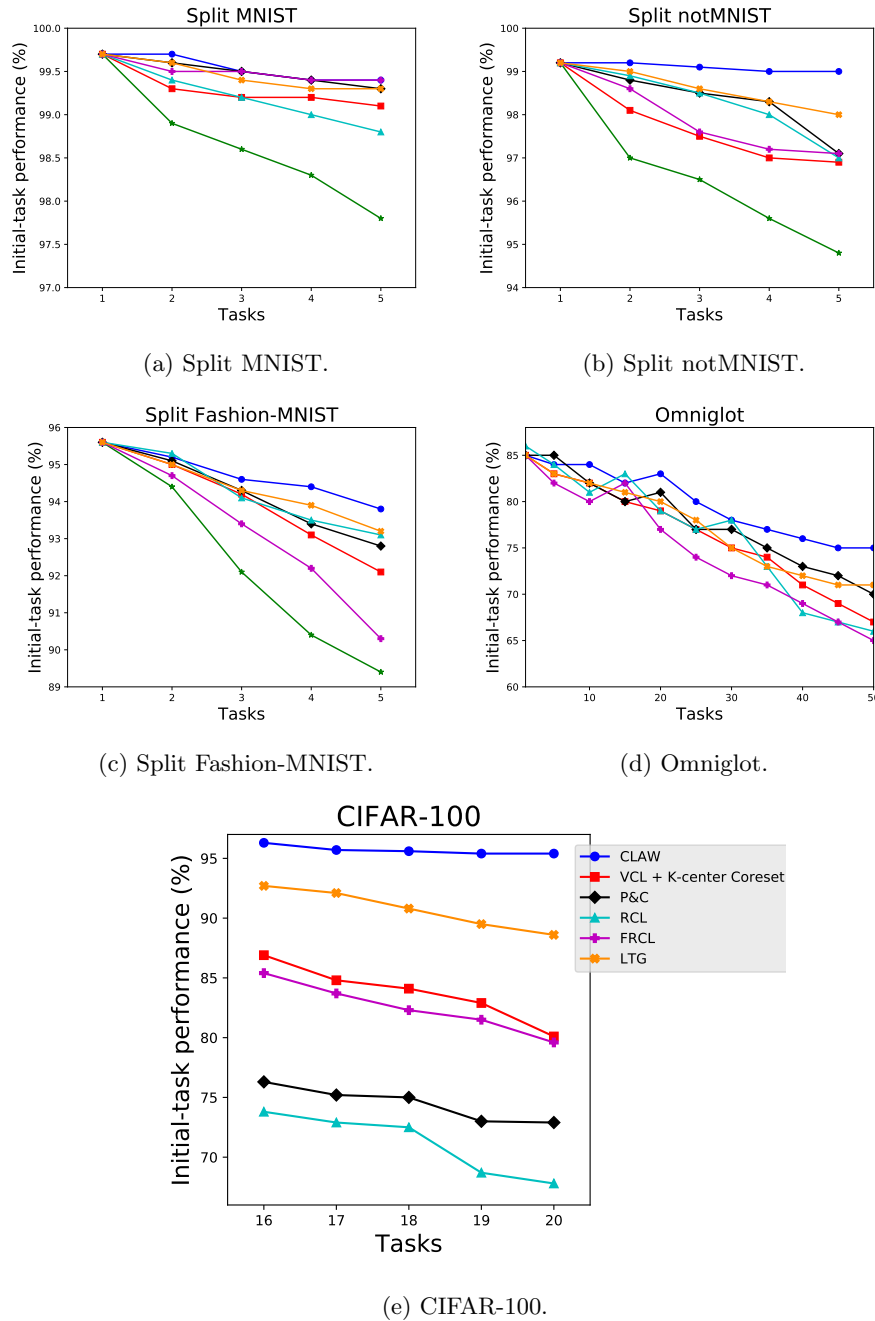
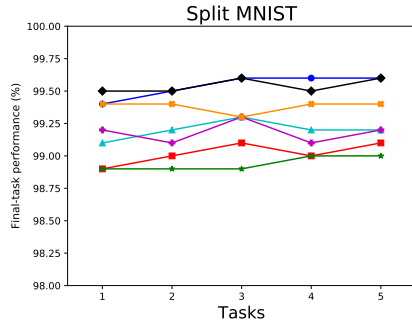
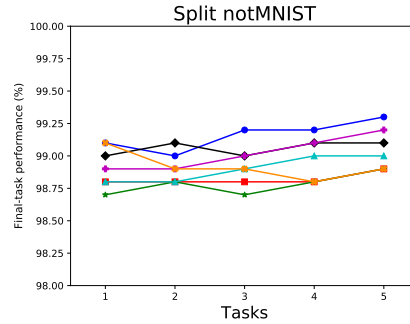


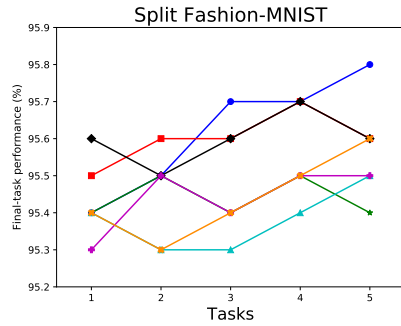
Figure 2: Evaluating catastrophic forgetting by measuring performance retention. Classification accuracy of the initial task is monitored along with the progression of tasks. Results are displayed for five datasets. **CLAW** is the least forgetful algorithm since performance levels achieved on the initial task do not degrade as much as in the other methods after facing new tasks. The legend and λ values for EWC are the same as in Figure 1. Best viewed in colour.



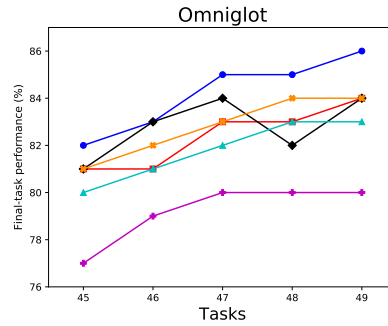
(a) Split MNIST.



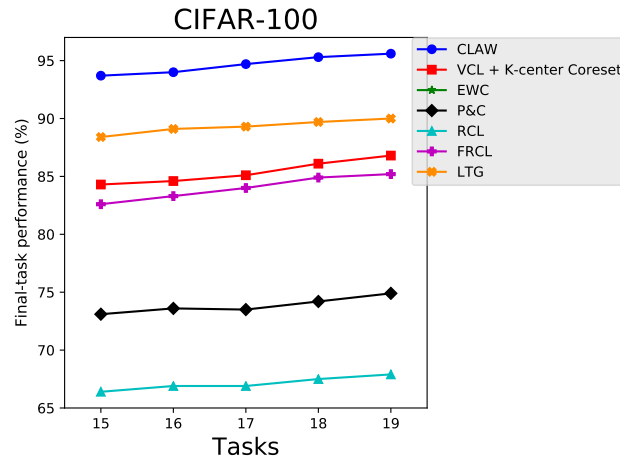
(b) Split notMNIST.



(c) Split Fashion-MNIST.



(d) Omniglot.



(e) CIFAR-100.

Figure 3: Evaluating Forward transfer, or to what extent a continual learning framework can avoid negative transfer. The impact of learning previous tasks on a specific task (the last task) is inspected and used as a proxy for evaluating forward transfer. This is performed by evaluating the relative performance achieved on a unique task after learning a varying number of previous tasks. This means that the value at $x\text{-axis} = 1$ refers to the learning accuracy of the last task after having learnt solely one task (only itself), the value at 2 refers to the learning accuracy of the last task after having learnt two tasks (an additional previous task), etc. Overall, **CLAW** achieves state-of-the-art results in 4 out of the 5 experiments (at par in the fifth) in terms of avoiding negative transfer. Best viewed in colour.

References

- Achille, A., Eccles, T., Matthey, L., Burgess, C., Watters, N., Lerchner, A., Higgins, I., 2018. Life-long disentangled representation learning with cross-domain latent homologies. *Advances in neural information processing systems (NIPS)*.
- Ahn, H., Lee, D., Cha, S., Moon, T., 2019. Uncertainty-based continual learning with adaptive regularization. *arXiv preprint arXiv:1905.11614*.
- Aljundi, R., Caccia, L., Belilovsky, E., Caccia, M., Lin, M., Charlin, L., Tuytelaars, T., 2019a. Online continual learning with maximally interfered retrieval. *Advances in neural information processing systems (NeurIPS)*.
- Aljundi, R., Lin, M., Goujaud, B., Bengio, Y., 2019b. Gradient based sample selection for online continual learning. *Advances in neural information processing systems (NeurIPS)*.
- Aljundi, R., Rohrbach, M., Tuytelaars, T., 2019c. Selfless sequential learning. *International Conference on Learning Representations (ICLR)*.
- Bakker, B., Heskes, T., 2003. Task clustering and gating for Bayesian multitask learning. *Journal of Machine Learning Research (JMLR)* 4, 83–99.
- Bernardo, J., Smith, A., 2000. *Bayesian theory*. John Wiley & Sons.
- Butalov, Y., 2011. The notMNIST dataset. <http://yaroslavvb.com/upload/notMNIST/>.
- Carpenter, G., Grossberg, S., 1987. A massively parallel architecture for a self-organizing neural pattern recognition machine. *Computer vision, graphics, and image processing* 37, 54–115.
- Caruana, R., 1997. Multi-task learning. *Machine Learning*.
- Chaudhry, A., Dokania, P., Ajanthan, T., Torr, P., 2018. Riemannian walk for incremental learning: Understanding forgetting and intransigence. *arXiv preprint arXiv:1801.10112*.

- Choi, E., Lee, K., Choi, K., 2019. Autoencoder-based incremental class learning without retraining on old data. arXiv preprint arXiv:1907.07872.
- Diaz-Rodriguez, N., Lomonaco, V., Filliat, D., Maltoni, D., 2018. Dont forget, there is more than forgetting: new metrics for Continual Learning. NIPS Continual Learning Workshop.
- Du, X., Charan, G., Liu, F., Cao, Y., 2019. Single-net continual learning with progressive segmented training (PST). arXiv preprint arXiv:1905.11550.
- Ebrahimi, S., Elhoseiny, M., Darrell, T., Rohrbach, M., 2019. Uncertainty-guided continual learning with Bayesian neural networks. arXiv preprint arXiv:1906.02425.
- Fernando, C., Banarse, D., Blundell, C., Zwols, Y., Ha, D., Rusu, A., Pritzel, A., Wierstra, D., 2017. PathNet: Evolution channels gradient descent in super neural networks. arXiv preprint arXiv:1701.08734.
- Finn, C., Abbeel, P., Levine, S., 2017. Model-agnostic meta-learning for fast adaptation of deep networks. International Conference on Machine Learning (ICML).
- French, R., 1999. Catastrophic forgetting in connectionist networks. Trends in cognitive sciences 3, 128–135.
- Ghosh, S., Yao, J., Doshi-Velez, F., 2018. Structured variational learning of Bayesian neural networks with horseshoe priors. International Conference on Machine Learning (ICML).
- Goodfellow, I., 2016. NIPS 2016 tutorial: Generative adversarial networks. arXiv preprint arXiv:1701.00160.
- Goodfellow, I., Mirza, M., Xiao, D., Courville, A., Bengio, Y., 2014a. An empirical investigation of catastrophic forgetting in gradient-based neural networks. International Conference on Learning Representations (ICLR).

- Goodfellow, I., Pouget-Abadie, J., Mirza, M., Xu, B., Warde-Farley, D., Ozair, S., Courville, A., Bengio, Y., 2014b. Generative adversarial nets. *Advances in neural information processing systems (NIPS)*, 2672–2680.
- Goodfellow, I., Warde-Farley, D., Mirza, M., Courville, A., Bengio, Y., 2013. Maxout networks. *International Conference on Machine Learning (ICML)*.
- Hattori, M., 2014. A biologically inspired dual-network memory model for reduction of catastrophic forgetting. *Neurocomputing* 134, 262–268.
- He, X., Sygnowski, J., Galashov, A., Rusu, A., Teh, Y. W., Pascanu, R., 2019. Task agnostic continual learning via meta learning. *arXiv preprint arXiv:1906.05201*.
- Heskes, T., 2000. Empirical Bayes for learning to learn.
- Hu, W., Lin, Z., Liu, B., Tao, C., Tao, Z., Ma, J., Zhao, D., Yan, R., 2019. Overcoming catastrophic forgetting via model adaptation. *International Conference on Learning Representations (ICLR)*.
- Isele, D., Cosgun, A., 2018. Selective experience replay for lifelong learning. *arXiv preprint arXiv:1802.10269*.
- Javed, K., White, M., 2019. Meta-learning representations for continual learning. *Advances in neural information processing systems (NeurIPS)*.
- Jung, H., Ju, J., Jung, M., Kim, J., 2016. Less-forgetting learning in deep neural networks. *arXiv preprint arXiv:1607.00122*.
- Kamra, N., Gupta, U., Liu, Y., 2017. Deep generative dual memory network for continual learning. *arXiv preprint arXiv:1710.10368*.
- Kaplanis, C., Shanahan, M., Clopath, C., 2018. Continual reinforcement learning with complex synapses. *International Conference on Machine Learning (ICML)*.

- Kemker, R., Kanan, C., 2018. FearNet: Brain-inspired model for incremental learnings. International Conference on Learning Representations (ICLR).
- Kemker, R., McClure, M., Abitino, A., Hayes, T., Kanan, C., 2018. Measuring catastrophic forgetting in neural networks. AAAI Conference on Artificial Intelligence 32.
- Kim, D., Bae, J., Jo, Y., Choi, J., 2019. Incremental learning with maximum entropy regularization: Rethinking forgetting and intransigence. arXiv preprint arXiv:1902.00829.
- Kim, H., Kim, S., Lee, J., 2018. Keep and learn: Continual learning by constraining the latent space for knowledge preservation in neural networks. MIC-CAI.
- Kingma, D., Ba, J., 2015. Adam: A Method for Stochastic Optimization. International Conference on Learning Representations (ICLR).
- Kingma, D., Rezende, D., Mohamed, S., Welling, M., 2014. Semi-supervised learning with deep generative models. Advances in neural information processing systems (NIPS) 28, 3581–3589.
- Kingma, D., Salimans, T., Welling, M., 2015. Variational dropout and the local reparameterization trick. Advances in neural information processing systems (NIPS), 2575–2583.
- Kirkpatrick, J., Pascanu, R., Rabinowitz, N., Veness, J., Desjardins, G., Rusu, A., Milan, K., Quan, J., Ramalho, T., Grabska-Barwinska, A., Hassabis, D., Clopath, C., Kumaran, D., Hadsell, R., 2017. Overcoming catastrophic forgetting in neural networks. Proceedings of the National Academy of Sciences (PNAS).
- Krizhevsky, A., Hinton, G., 2009. Learning multiple layers of features from tiny images. Technical Report, University of Toronto.

- Lake, B., Salakhutdinov, R., Gross, J., Tenenbaum, J., 2011. One shot learning of simple visual concepts. *Proceedings of the Cognitive Science Society* 33.
- LeCun, Y., Bottou, L., Bengio, Y., Haffner, P., 1998. Gradient-based learning applied to document recognition. In *Proceedings of the IEEE* 86 (11), 2278–2324.
- Lee, S., Kim, J., Jun, J., Ha, J., Zhang, B., 2017. Overcoming catastrophic forgetting by incremental moment matching. *Advances in neural information processing systems (NIPS)*.
- Li, H., Enshaeifar, S., Ganz, F., Barnaghi, P., 2019a. Continual learning in deep neural network by using a Kalman optimiser. *ICML Workshop*.
- Li, X., Zhou, Y., Wu, T., Socher, R., Xiong, C., 2019b. Learn to grow: A continual structure learning framework for overcoming catastrophic forgetting. *International Conference on Machine Learning (ICML)*.
- Li, Z., Hoiem, D., 2016. Learning without forgetting. *European Conference on Computer Vision (ECCV)*.
- Lin, M., Fu, J., Bengio, Y., 2018. Conditional computation for continual learning. *NIPS Continual Learning Workshop*.
- Lopez-Paz, D., Ranzato, M., 2017. Gradient episodic memory for continual learning. *Advances in neural information processing systems (NIPS)*.
- Louizos, C., Ullrich, K., Welling, M., 2017. Bayesian compression for deep learning. *Advances in neural information processing systems (NIPS)*, 3288–3298.
- McCloskey, M., Cohen, N., 1989. Catastrophic interference in connectionist networks: The sequential learning problem. *Psychology of Learning and Motivation*.
- Mocanu, D., Vega, M., Eaton, E., Stone, P., Liotta, A., 2016. Online contrastive divergence with generative replay: Experience replay without storing data. *arXiv preprint arXiv:1610.05555*.

- Molchanov, D., Ashukha, A., Vetrov, D., 2017. Variational dropout sparsifies deep neural networks. *International Conference on Machine Learning (ICML)*, 2498–2507.
- Nguyen, C., Li, Y., Bui, T., Turner, R., 2018. Variational continual learning. *International Conference on Learning Representations (ICLR)*.
- Ostapenko, O., Puscas, M., Klein, T., Jahnichen, P., Nabi, M., 2019. Learning to remember: A synaptic plasticity driven framework for continual learning. *Proceedings of the IEEE Conference on Computer Vision and Pattern Recognition (CVPR)*.
- Pape, L., Gomez, F., Ring, M., Schmidhuber, J., 2011. Modular deep belief networks that do not forget. *IEEE International Joint Conference on Neural Networks (IJCNN)*.
- Parisi, G., Kemker, R., Part, J., Kanan, C., Wermter, S., 2019. Continual lifelong learning with neural networks: A review. *Neural Networks*.
- Park, D., Hong, S., Han, B., Lee, K., 2019. Continual learning by asymmetric loss approximation with single-side overestimation. *arXiv preprint arXiv:1908.02984*.
- Pfulb, B., Gepperth, A., 2019. A comprehensive, application-oriented study of catastrophic forgetting in DNNs. *International Conference on Learning Representations (ICLR)*.
- Rajasegaran, J., Hayat, M., Khan, S., Khan, F., Shao, L., 2019. Random path selection for incremental learning. *Advances in neural information processing systems (NeurIPS)*.
- Ratcliff, R., 1990. Connectionist models of recognition memory: Constraints imposed by learning and forgetting functions. *Psychological Review*.
- Rebuffi, S., Kolesnikov, A., Sperl, G., Lampert, C., 2017. iCaRL: Incremental classifier and representation learning. *Proceedings of the IEEE Conference on Computer Vision and Pattern Recognition (CVPR)*.

- Riemer, M., Cases, I., Ajemian, R., Liu, M., I.Rish, Tu, Y., Tesauro, G., 2019. Learning to learn without forgetting by maximizing transfer and minimizing interference. International Conference on Learning Representations (ICLR).
- Ring, M., 1995. Continual learning in reinforcement environments. Ph.D. thesis, University of Texas, Austin.
- Ring, M., 1997. CHILD: A first step towards continual learning. Machine Learning.
- Robins, A., 1993. Catastrophic forgetting in neural networks: The role of rehearsal mechanisms. IEEE Artificial Neural Networks and Expert Systems, 65–68.
- Robins, A., 1995. Catastrophic forgetting, rehearsal and pseudorehearsal. Connection Science 7, 123–146.
- Rolnick, D., Ahuja, A., Schwarz, J., Lillicrap, T., Wayne, G., 2018. Experience replay for continual learning. arXiv preprint arXiv:1811.11682.
- Rusu, A., Rabinowitz, N., Desjardins, G., Soyer, H., Kirkpatrick, J., Kavukcuoglu, K., Pascanu, R., Hadsell, R., 2016a. Progressive neural networks. arXiv preprint arXiv:1606.04671.
- Rusu, A., Vecerik, M., Rothoerl, T., Heess, N., Pascanu, R., Hadsell, R., 2016b. Sim-to-Real robot learning from pixels with progressive nets. arXiv preprint arXiv:1610.04286.
- Schlimmer, J., Fisher, D., 1986. A case study of incremental concept induction. The National Conference on Artificial Intelligence.
- Schmidhuber, J., 2013. Powerplay: Training an increasingly general problem solver by continually searching for the simplest still unsolvable problem. Frontiers in psychology 4.
- Schmidhuber, J., 2018. One big net for everything. arXiv preprint arXiv:1802.08864.

- Schwarz, J., Luketina, J., Czarnecki, W., Grabska-Barwinska, A., Teh, Y. W., Pascanu, R., Hadsell, R., 2018. Progress & compress: A scalable framework for continual learning. International Conference on Machine Learning (ICML).
- Serra, J., Suris, D., Miron, M., Karatzoglou, A., 2018. Overcoming catastrophic forgetting with hard attention to the task. International Conference on Machine Learning (ICML).
- Shin, H., Lee, J., Kim, J., Kim, J., 2017. Continual learning with deep generative replay. Advances in neural information processing systems (NIPS).
- Srivastava, N., Hinton, G., Krizhevsky, A., Sutskever, I., Salakhutdinov, R., 2014. Dropout: A simple way to prevent neural networks from overfitting. Journal of Machine Learning Research (JMLR) 15, 1929–1958.
- Srivastava, R., Masci, J., Kazerounian, S., Gomez, F., Schmidhuber, J., 2013. Compete to compute. Advances in neural information processing systems (NIPS).
- Stickland, A., Murray, I., 2019. BERT and PALs: Projected attention layers for efficient adaptation in multi-task learning. International Conference on Machine Learning (ICML).
- Sutton, R., Whitehead, S., 1993. Online learning with random representations. International Conference on Machine Learning (ICML).
- Swietojanski, P., Renals, S., 2014. Learning hidden unit contributions for unsupervised speaker adaptation of neural network acoustic models. IEEE Spoken Language Technology Workshop (SLT).
- Teng, D., Dasgupta, S., 2019. Continual learning via online leverage score sampling. arXiv preprint arXiv:1908.00355.
- Thrun, S., 1996. Explanation-based neural network learning: A lifelong learning approach. Springer Science & Business Media 357.

- Titsias, M., Schwarz, J., Matthews, A., Pascanu, R., Teh, Y. W., 2019. Functional regularisation for continual learning using Gaussian processes. arXiv preprint arXiv:1901.11356.
- van de Ven, G., Tolias, A., 2018. Generative replay with feedback connections as a general strategy for continual learning. arXiv preprint arXiv:1809.10635.
- Vuorio, R., Cho, D., Kim, D., Kim, J., 2018. Meta continual learning. arXiv preprint arXiv:1806.06928.
- Wu, C., Herranz, L., Liu, X., Wang, Y., van de Weijer, J., Raducanu, B., 2018. Memory replay GANs: Learning to generate new categories without forgetting. Advances in neural information processing systems (NIPS).
- Xiao, H., Rasul, K., Vollgraf, R., 2017. Fashion-MNIST: a novel image dataset for benchmarking machine learning algorithms. arXiv preprint arXiv:1708.07747.
- Xu, J., Ma, J., Zhu, Z., 2019. Bayesian Optimized Continual Learning with Attention Mechanism. arXiv preprint arXiv:1905.03980.
- Xu, J., Zhu, Z., 2018. Reinforced continual learning. Advances in neural information processing systems (NIPS).
- Yoon, J., Kim, S., Yang, E., Hwang, S., 2019. ORACLE: Order robust adaptive continual learning. arXiv preprint arXiv:1902.09432.
- Yoon, J., Yang, E., Lee, J., Hwang, S., 2018. Lifelong learning with dynamically expandable networks. International Conference on Learning Representations (ICLR).
- Zenke, F., Poole, B., Ganguli, S., 2017. Continual learning through synaptic intelligence. International Conference on Machine Learning (ICML).
- Zeno, C., Golan, I., Hoffer, E., Soudry, D., 2018. Task agnostic continual learning using online variational Bayes. NIPS Bayesian Deep Learning Workshop.

Appendix

We begin by briefly summarising the contents of the Appendix below:

- Related works are described in Section Appendix A, followed by a brief discussion on the potential applicability of CLAW to another continual learning (CL) framework in Section Appendix A.1.
- In Section Appendix B, we provide the statistical significance and standard error of the average classification accuracy results obtained after completing the last two tasks from each experiment.
- Further experimental details are given in Section Appendix C.
- In Section Appendix D and Figures D.4- D.8, we display the results of performed ablations which manifest the relevance of each adaptation parameter.

Appendix A. Related Work

A complementary approach to CLAW, which could be combined with it, is the regularisation-based approach to balance adaptability with catastrophic forgetting: a level of stability is kept via protecting parameters that greatly influence the prediction against radical changes, while allowing the rest of the parameters to change without restriction (Li and Hoiem, 2016; Vuorio et al., 2018). In (Zenke et al., 2017), the regulariser is based on synapses where an importance measure is locally computed at each synapse during training, based on their respective contributions to the change in the global loss. During a task change, the less important synapses are given the freedom to change whereas catastrophic forgetting is avoided by preventing the important synapses from changing (Zenke et al., 2017). The elastic weight consolidation (EWC) algorithm, introduced by Kirkpatrick et al. (2017), is a seminal example of this approach where a quadratic penalty is imposed on the difference between parameter values of the old and new tasks. One limitation of EWC, which is

rather alleviated by using minibatch or stochastic estimates, appears when the output space is not low-dimensional, since the diagonal of the Fisher information matrix over parameters of the old task must be computed, which requires a summation over all possible output labels (Kirkpatrick et al., 2017; Zenke et al., 2017; Schwarz et al., 2018). In addition, the regularisation term involves a sum over all previous tasks with a term from each and a hand-tuned hyperparameter that alters the weight given to it. The accumulation of this leads to a lot of hand-tuning. The work in (Chaudhry et al., 2018) is based on penalising confident fitting to the uncertain knowledge by a maximum entropy regulariser.

Another seminal algorithm based on regularisation, which can be applied to any model, is variational continual learning (VCL) (Nguyen et al., 2018) which formulates CL as a sequential approximate (variational) inference problem. However, VCL has only been applied to simple architectures, not involving any automatic model building or adaptation. The framework in (Lee et al., 2017) incrementally matches the moments of the posterior of a Bayesian neural network that has been trained on the first and then the second task, and so on. Other algorithms pursue regularisation approaches based on sparsity (Srivastava et al., 2013; Kim et al., 2018). For example, the work in (Aljundi et al., 2019c) encourages sparsity on the neuron activations to alleviate catastrophic forgetting. The l_2 distance between the top hidden activations of the old and new tasks is used for regularisation in (Jung et al., 2016). This approach has achieved good results, but is computationally expensive due to the necessity of computing at least a forward pass for every new data point through the network representing the old task (Zenke et al., 2017). Other regularisation-based continual learning algorithms include (Ebrahimi et al., 2019; Park et al., 2019).

Another approach is the architecture-based one where the principal aim is to administer both the stability and adaptation issues via dividing the architecture into reusable parts that are less prone to changes, and other parts especially devoted to individual tasks (Rusu et al., 2016b; Fernando et al., 2017; Yoon et al., 2018; Du et al., 2019; He et al., 2019; Li et al., 2019a; Xu et al., 2019). To learn a new task in the work by Rusu et al. (2016a), the whole network from

the previous task is first copied then augmented with a new part of the architecture. Although this is effective in eradicating catastrophic forgetting, there is a clear scalability issue since the architecture growth can be prohibitively high, especially with an increasing number of tasks. The work introduced in (Li et al., 2019b) bases its continual learning on neural architecture search, whereas the representation in (Javed and White, 2019) is optimised such that online updates minimize the error on all samples while limiting forgetting. The framework proposed by Xu and Zhu (2018) interestingly aims at solving this neural architecture structure learning problem, while balancing the tradeoff between adaptation and stability, via designed reinforcement learning (RL) strategies. When facing a new task, the optimal number of neurons and filters to add to each layer is cast as a combinatorial optimisation problem solved by an RL strategy whose reward signal is a function of validation accuracy and network complexity. Another RL based framework is the one presented by Kaplanis et al. (2018) where catastrophic forgetting is mitigated at multiple time scales via RL agents with a synaptic model inspired by neuroscience. Bottom layers (those near the input) are generally shared among the different tasks, while layers near the output are task-specific. Since the model structure is usually divided a priori and no automatic architecture learning nor adaptation takes place, alteration on the shared layers can still cause performance loss on earlier tasks due to forgetting (Shin et al., 2017). A clipped version of maxout networks (Goodfellow et al., 2013) is developed in (Lin et al., 2018) where parameters are partially shared among examples. The method in (Ostapenko et al., 2019) is based a dynamic network expansion accomplished by a generative adversarial network.

The memory-based approach, which is the third influential approach to address the adaptation-catastrophic forgetting tradeoff, relies on episodic memory to store data (or pseudodata) from previous tasks (Ratcliff, 1990; Robins, 1993, 1995; Hattori, 2014; Rolnick et al., 2018; Teng and Dasgupta, 2019). A major limitation of the memory-based approach is that data from previous tasks may not be available in all real-world problems (Shin et al., 2017; Choi et al., 2019).

Another limitation is the overhead resulting from the memory requirements, e.g. storage, replay, etc. In addition, the optimisation required to select the best observation to replay for future tasks is a source of further overhead (Titsias et al., 2019). In addition to the explicit replay form, some works have been based on generative replay (Thrun, 1996; Schmidhuber, 2013; Mocanu et al., 2016; Rebuffi et al., 2017; Kamra et al., 2017; Shin et al., 2017; van de Ven and Tolias, 2018; Wu et al., 2018). Notably, Shin et al. (2017) train a deep generative model based on generative adversarial networks (GANs, Goodfellow et al., 2014b; Goodfellow, 2016) to mimic past data. This mitigates the aforementioned problem, albeit at the added cost of the training of the generative model (Schwarz et al., 2018) and sharing its parameters. Alleviating catastrophic forgetting via replay mechanisms has also been adopted in reinforcement learning, e.g. (Isele and Cosgun, 2018; Rolnick et al., 2018). A similar approach was introduced by Lopez-Paz and Ranzato (2017) where gradients of the previous task (rather than data examples) are stored so that a trust region consisting of gradients of all previous tasks can be formed to reduce forgetting. Other algorithms based on replay mechanisms include (Aljundi et al., 2019a,b).

Equivalent tradeoffs to the one between adaptation and stability can be found in the literature since the work in (Carpenter and Grossberg, 1987), in which a balance was needed to resolve the stability-plasticity dilemma, where the latter refers to the ability to rapidly adapt to new tasks. The works introduced in (Chaudhry et al., 2018; Kim et al., 2019) shed light on the tradeoff between adaptation and stability, where they explore measures of intransigence and forgetting. The former refers to the inability to adapt to new tasks and data, whereas an increase in the latter clearly signifies an instability problem. Other recent works tackling the same tradeoff include (Riemer et al., 2019) where the transfer-interference (interference is catastrophic forgetting) tradeoff is optimised for the sake of maximising transfer and minimising interference by an algorithm based on experience replay and meta-learning. Other recent algorithms include the ORACLE algorithm by Yoon et al. (2019), which addresses the sensitivity of a continual learner to the order of tasks it encounters by es-

establishing an order robust learner that represents the parameters of each task as a sum of task-shared and task-specific parameters. The algorithm in (Titsias et al., 2019) achieves functional regularisation by performing approximate inference over the function (instead of parameter) space. They use a Gaussian process obtained by assuming the weights of the last neural network layer to be Gaussian distributed. Our model is also related to the multi-task learning approach (Caruana, 1997; Heskes, 2000; Bakker and Heskes, 2003; Stickland and Murray, 2019).

Appendix A.1. Applicability of CLAW to Other CL Frameworks

As mentioned in the main document, ideas of the proposed CLAW can be applied to continual learning frameworks other than VCL. The latter is more relevant for the inference part of CLAW since both are based on variational inference. As per the modeling ideas, e.g. the binary adaptation parameter depicting whether or not to adapt, and the maximum allowed adaptation, these can be integrated within other continual learning frameworks. For example, the algorithm in Xu and Zhu (2018) utilises reinforcement learning to adaptively expand the network. The optimal number of nodes and filters to be added is cast as a combinatorial optimisation problem. In CLAW, we do not expand the network. As such, an extension of the work in (Xu and Zhu, 2018) can be inspired by CLAW where not only the number of nodes and filters to be added is decided for each task, but also a soft and more general version where an adaptation based on the same network size is performed such that the network expansion needed in (Xu and Zhu, 2018) can be further moderated.

Appendix B. Statistical Significance and Standard Error

In this section, we provide information about the statistical significance and standard error of CLAW and the competing continual learning frameworks. In Table B.1, we list the average accuracy values (Figure 1 in the main document) obtained after completing the last two tasks from each of the six experiments. A

bold entry in Table B.1 denotes that the classification accuracy of an algorithm is significantly higher than its competitors. Significance results are identified using a paired t-test with $p = 0.05$. Each average accuracy value is followed by the corresponding standard error. Average classification accuracy resulting from **CLAW** is significantly higher than its competitors on the 6 experiments.

Table B.1: Average test classification accuracy of the last two tasks in each of the six experiments: Permuted MNIST, Split MNIST, Split notMNIST, Split Fashion-MNIST, Omniglot and CIFAR-100, followed by the corresponding standard error. A bold entry denotes that the classification accuracy of an algorithm is significantly higher than its competitors. Significance results are identified using a paired t-test with $p = 0.05$. Average classification accuracy resulting from **CLAW** is significantly higher than its competitors on the 6 experiments.

Classification accuracy	CLAW	VCL	VCL + Coreset	EWC	P&C	RCL	FRCL	LTG
Permuted MNIST (task 9)	99.2 ± 0.2 %	93.5 ± 0.3 %	95.5 ± 0.3 %	92.1 ± 0.4 %	94.4 ± 0.3 %	96.4 ± 0.5 %	98.4 ± 0.4 %	98.7 ± 0.3 %
Permuted MNIST (task 10)	99.2 ± 0.1 %	92.1 ± 0.3 %	95 ± 0.5 %	90.2 ± 0.4 %	94.1 ± 0.6 %	96.3 ± 0.3 %	98.4 ± 0.5 %	98.65 ± 0.3 %
Split MNIST (task 4)	99.2 ± 0.2 %	98.6 ± 0.3 %	98.7 ± 0.2 %	94.9 ± 0.4 %	97.3 ± 0.5 %	97.8 ± 0.7 %	98.2 ± 0.3 %	98.7 ± 0.2 %
Split MNIST (task 5)	99.1 ± 0.2 %	97.0 ± 0.4 %	98.4 ± 0.3 %	94.2 ± 0.5 %	96.4 ± 0.4 %	97.5 ± 0.6 %	98.1 ± 0.2 %	98.3 ± 0.3 %
Split notMNIST (task 4)	98.7 ± 0.3 %	95.8 ± 0.4 %	96.9 ± 0.5 %	92.9 ± 0.4 %	97.8 ± 0.4 %	97.7 ± 0.2 %	96.1 ± 0.6 %	97.8 ± 0.3 %
Split notMNIST (task 5)	98.4 ± 0.2 %	92.1 ± 0.3 %	96.0 ± 0.3 %	92.3 ± 0.4 %	96.9 ± 0.5 %	97.3 ± 0.5 %	95.2 ± 0.7 %	97.4 ± 0.3 %
Split Fashion-MNIST (task 4)	93.2 ± 0.2 %	90.0 ± 0.3 %	90.7 ± 0.2 %	89.4 ± 0.4 %	91.4 ± 0.3 %	91.1 ± 0.3 %	90.4 ± 0.2 %	92.5 ± 0.4 %
Split Fashion-MNIST (task 5)	92.5 ± 0.2 %	88.0 ± 0.2 %	88.5 ± 0.4 %	87.6 ± 0.3 %	90.8 ± 0.2 %	89.7 ± 0.4 %	87.7 ± 0.4 %	91.1 ± 0.3 %
Omniglot (task 49)	84.5 ± 0.2 %	81.1 ± 0.3 %	81.8 ± 0.3 %	78.2 ± 0.3 %	82.8 ± 0.2 %	80.1 ± 0.4 %	79.9 ± 0.3 %	83.6 ± 0.3 %
Omniglot (task 50)	84.6 ± 0.3 %	80.7 ± 0.3 %	81.1 ± 0.4 %	77.3 ± 0.3 %	82.7 ± 0.3 %	80.2 ± 0.4 %	79.8 ± 0.5 %	83.5 ± 0.3 %
CIFAR-100 (task 19)	95.6 ± 0.3 %	78.7 ± 0.4 %	80.8 ± 0.3 %	63.1 ± 0.5 %	68.3 ± 0.6 %	63.7 ± 0.6 %	77.4 ± 0.7 %	86.2 ± 0.4 %
CIFAR-100 (task 20)	95.6 ± 0.3 %	77.2 ± 0.4 %	79.9 ± 0.4 %	62.4 ± 0.4 %	65.5 ± 0.6 %	60.4 ± 0.6 %	76.8 ± 0.6 %	85.6 ± 0.5 %

Appendix C. Other Experimental Details

Here are some additional details about the datasets in use:

The **MNIST** dataset is used in both the Permuted MNIST and Split MNIST experiments. The MNIST (Mixed National Institute of Standards and Technology) dataset (LeCun et al., 1998) is a handwritten digit dataset. Each MNIST image consists of 28×28 pixels, which is also the pixel size of the notMNIST and Fashion-MNIST datasets. The MNIST dataset contains a training set of

60,000 instances and a test set of 10,000 instances.

As mentioned in the main document, each experiment is repeated ten times. Data is randomly split into three partitions, training, validation and test. A portion of 60% of the data is reserved for training, 20% for validation and 20% for testing. Statistics reported are the averages of these ten repetitions.

Number of epochs required per task to reach a saturation level for **CLAW** (and the bulk of the methods in comparison) was 10 epochs for all experiments except for Omniglot and CIFAR-100 (15 epochs). Used values of ω_1 and ω_2 are 0.05 and 0.02, respectively.

For Omniglot, we used a network similar to the one used in (Schwarz et al., 2018), which consists of 4 blocks of 3×3 convolutions with 64 filters, followed by a ReLU and a 2×2 max-pooling. The same CNN is used for CIFAR-100. **CLAW** achieves clearly higher classification accuracy on both Omniglot and CIFAR-100 (Figures 1e and 1f).

Appendix D. Ablations

The plots displayed in this section empirically demonstrate how important the main adaptation parameters are in achieving the classification performance levels reached by **CLAW**. In each of the Figures D.4- D.9, the classification performance of **CLAW** is compared to the following three cases: 1) when the parameter controlling the maximum degree of adaptation is not learnt in a multi-task fashion, i.e. when the respective general value $\mathbf{s}_{i,j}$ is used instead of $\mathbf{s}_{i,j,t}$. 2) when adaptation always happens, i.e. the binary variable denoting the adaptation decision is always activated. 3) when adaptation never takes place. The differences in classification accuracy between **CLAW** and each of the other three plots in Figures D.4- D.9 empirically demonstrate the relevance of each adaptation parameter.

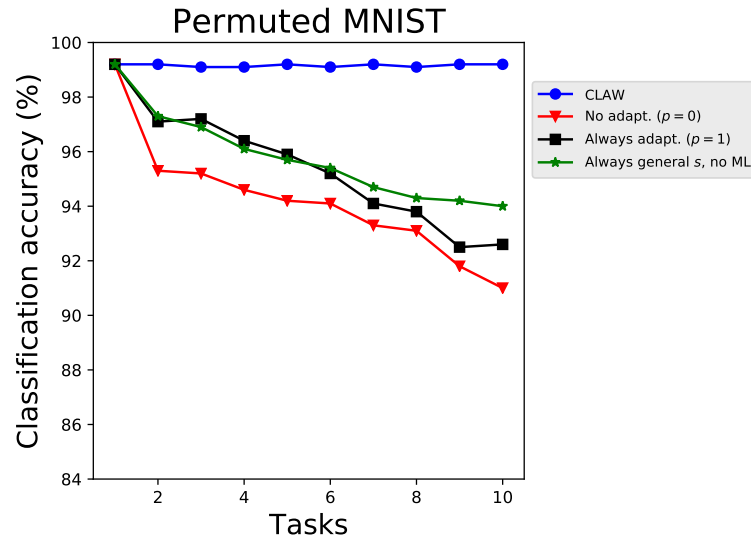


Figure D.4: Ablations for Permuted MNIST.

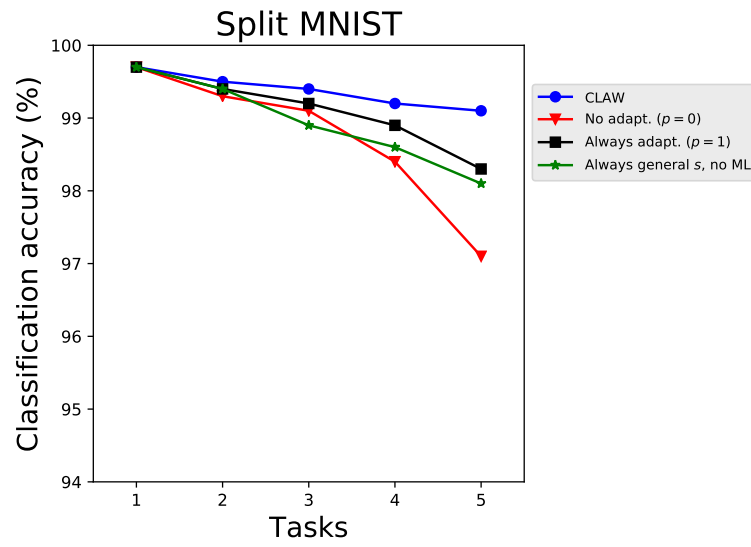


Figure D.5: Ablations for Split MNIST.

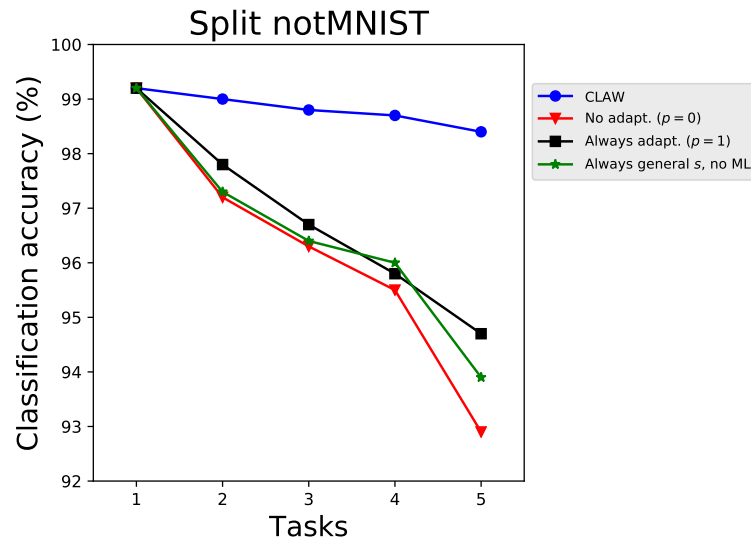


Figure D.6: Ablations for Split notMNIST.

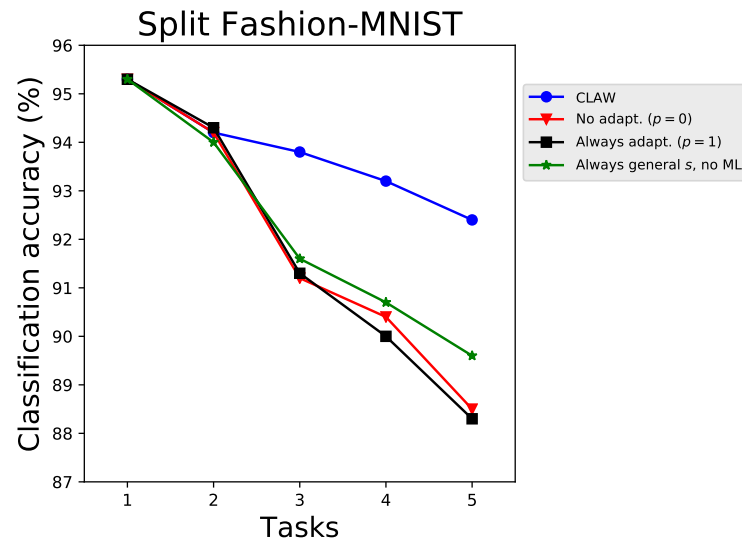


Figure D.7: Ablations for Split Fashion-MNIST.

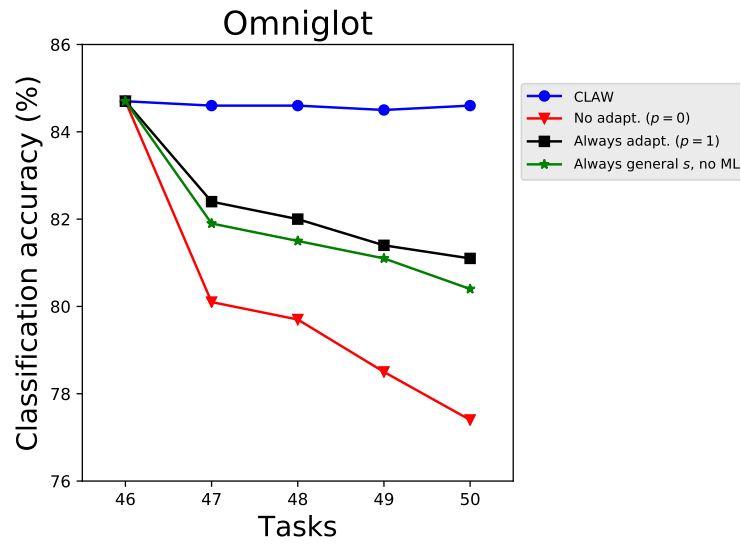


Figure D.8: Ablations for Omniglot.

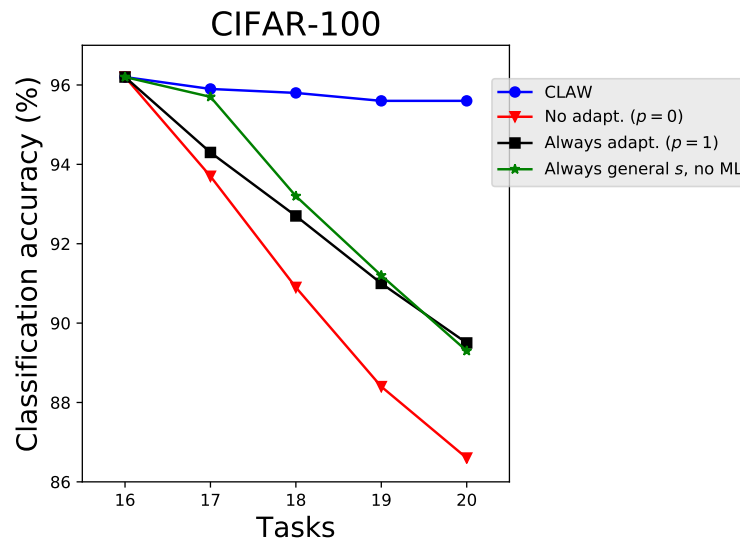


Figure D.9: Ablations for CIFAR-100.